Biofilm 7 (2024) 100176

Contents lists available at ScienceDirect

Biofilm

journal homepage: www.sciencedirect.com/journal/biofilm

Evaluating a polymicrobial biofilm model for structural components by co-culturing *Komagataeibacter hansenii* produced bacterial cellulose with *Pseudomonas aeruginosa* PAO1

Usha Rani Mahadevaswamy [a], Sudarsan Mugunthan [b], Thomas Seviour [b,c,1,**], Staffan Kjelleberg [b,d,e], Sierin Lim [a,f,*]

[a] School of Chemistry, Chemical Engineering and Biotechnology, Nanyang Technological University, Singapore
[b] Singapore Centre for Environmental Life Sciences Engineering, Nanyang Technological University, Singapore
[c] Centre for Water Technology (WATEC), Department of Biological and Chemical Engineering, Aarhus University, Aarhus, 8000, Denmark
[d] School of Biological Sciences, Nanyang Technological University, Singapore
[e] School of Biological, Earth and Environmental Sciences, University of New South Wales, Sydney, Australia
[f] Nanyang Environment and Water Research Institute, Nanyang Technological University, Singapore

ARTICLE INFO

Keywords:
Biofilm
Co-culture
Structural integration
EPS
Extracellular DNA
Microbial population
Komagataeibacter hansenii
Pseudomonas aeruginosa PAO1

ABSTRACT

A polymicrobial biofilm model of *Komagataeibacter hansenii* and *Pseudomonas aeruginosa* was developed to understand whether a pre-existing matrix affects the ability of another species to build a biofilm. *P. aeruginosa* was inoculated onto the preformed *K. hansenii* biofilm consisting of a cellulose matrix. *P. aeruginosa* PAO1 colonized and infiltrated the *K. hansenii* bacterial cellulose biofilm (BC), as indicated by the presence of cells at 19 μm depth in the translucent hydrogel matrix. Bacterial cell density increased along the imaged depth of the biofilm (17-19 μm). On day 5, the average bacterial count across sections was 67 ± 4 % *P. aeruginosa* PAO1 and 33 ± 6 % *K. hansenii*. Biophysical characterization of the biofilm indicated that colonization by *P. aeruginosa* modified the biophysical properties of the BC matrix, which inlcuded increased density, heterogeneity, degradation temperature and thermal stability, and reduced crystallinity, swelling ability and moisture content. This further indicates colonization of the biofilm by *P. aeruginosa.* While eDNA fibres - a key viscoelastic component of *P. aeruginosa* biofilm - were present on the surface of the co-cultured biofilm on day 1, their abundance decreased over time, and by day 5, no eDNA was observed, either on the surface or within the matrix. *P. aeruginosa*-colonized biofilm devoid of eDNA retained its mechanical properties. The observations demonstrate that a pre-existing biofilm scaffold of *K. hansenii* inhibits *P. aeruginosa* PAO1 eDNA production and suggest that eDNA production is a response by *P. aeruginosa* to the viscoelastic properties of its environment.

1. Introduction

Biofilms are an adaptation enabling microbial survival under a broad range of environmental conditions [1,2], an important mode of microbial life that play vital structural and functional roles [3,4]. Microbes achieve the formation of biofilm by secreting exopolymers that promote phase separation and the establishment of a physically distinct habitat for cells, that is the extracellular matrix [5]. This provides the microbes with a defense mechanism, where cells are encased within extracellular polymeric substance (EPS) thereby enabling adhesion to surfaces, nutrient sequestration, increased persistence, passaging of signaling molecules and other virulence factors, genetic exchange, creation of microenvironments, increased mechanical stability, and antimicrobial tolerance [6,7]. Numerous aspects of biofilms, including quorum sensing, growth mechanisms, virulence, extracellular polymers and matrix building, have been studied extensively in single species systems (e.g., *Pseudomonas aeruginosa*) [8]. However, in clinical and environmental systems, bacteria rarely exist in pure cultures. Instead,

* Corresponding author.
** Corresponding author. Singapore Centre for Environmental Life Sciences Engineering, Nanyang Technological University, Singapore.
E-mail addresses: twseviour@bce.au.dk (T. Seviour), SLim@ntu.edu.sg (S. Lim).
[1] Present address: Department of Biological and Chemical Engineering - Environmental Technology Engineering & Centre for Water Technology (WATEC), BCE, Aarhus University, Denmark.

https://doi.org/10.1016/j.bioflm.2024.100176
Received 20 July 2023; Received in revised form 21 December 2023; Accepted 4 January 2024
Available online 6 January 2024

polymicrobial communities predominate, where a range of relationships can exist between constituent populations [9,10].

The effects of community interactions within biofilms vary widely, from enhancing growth and survival of some, to inhibiting growth or killing another. *Pseudomonads* are present in many ecological settings. While *P. aeruginosa* has been shown to have an antagonistic relationship with some species, such as filamentous *Candida albicans,* which it attacks and kills, it neither attaches to nor kills others like yeast-form cells [11]. Competitive interactions can occur in community biofilms, due to overlapping metabolic preferences. Co-operative interactions are also possible which can contribute to enhanced biomass and biopolymer production [12,13]. Biofilms provide a matrix for localized interactions between species. Our understanding of polymicrobial EPS composition, its functional role, structural organization, ultimately how different microbes collectively regulate production and interact with EPS components within biofilm, is limited. Understanding the ecological roles and relationships between microbial populations in community biofilms is important to develop novel strategies to control biofilm formation.

In this study, two well-known biofilm formers *K. hansenii* and *P. aeruginosa PAO1* were used. Studies on co-culturing of BC-producing strains with other microorganisms are scarce. *P. aeruginosa* is a well-characterized model microorganism for studying biofilm formation and is commonly used to address questions about biofilm biology and ecology in general. It is actively motile in a wide-range of growth temperatures (25-42 °C), pH (5.6–9) and has simple nutritional requirements [14]. It is also well understood in terms of matrix composition having several polysaccharides in matrix formation (i.e., alginate, Pel and Psl) as well as proteins (CdrA, type iV fimbriae, functional amyloids), eDNA [15] and eRNA [16] as foundation structural polymers in its biofilms.

eDNA was first observed in biofilms around twenty years ago [17]. Recently, attention has been diverted to the mechanism of eDNA assembly in the matrix and its formation. Some researchers indicate that it results from programmed lytic explosion of cells, others that it is the unplanned consequence of cell lysis [18]. A third explanation is that it is coordinated by quorum sensing [15]. Following release, it assembles into a 3-D cross-linked network that contributes to the foundation structure of *Pseudomonas* biofilm matrices. Turnbull *et al.*, 2016*,* illustrated that coordinated explosive cell lysis occurred with a specific subpopulation of *P. aeruginosa* resulting in eDNA release and matrix assembly [18]. Furthermore, DNase has been shown to be effective at inhibiting biofilm formation at early stages of growth, but has no significant effects on established biofilms. This is likely due to the effect of protective interactions within the biofilm matrix [17,19], for example, resulting from crosslinking of eDNA by the cationic exopolysaccharide Pel [20], the formation of G-quadreplex eDNA structures [21], shielding of the eDNA from enzymatic actions [19] through the transition from B- to Z-form DNA [22], or hybrid formation with eRNA in the matrix [16]. However, what triggers the transition of supercoiled chromosomal DNA to viscoelastic and networked eDNA is not understood, including whether it is an active or deliberate strategy by the bacteria to assemble a biofilm matrix. We therefore sought to address this question, and specifically whether eDNA production by *P. aeruginosa* still occurs under conditions when a foundational matrix sub-structure is not required, such as when it colonizes another biofilm.

Bacterial cellulose (BC) produced by *Komagataeibacter* spp. (formerly *Gluconacetobacter*) was used as primary scaffold due to its unique characteristics such as nanofibrous, porous, crystalline matrix making it stand out over cellulose from other sources [23]. To the authors best knowledge, there are no studies reporting the presence of eDNA as key structural material in *K. hansenii* biofilms and thus an ideal model to investigate the research hypothesis. Using BC as a model preformed matrix allows an assessment of whether eDNA is a passive mechanism or an active response to the need for a biofilm matrix structure. Furthermore, this study demonstrates the value of the *Komagataeibacter* spp. and *P. aeruginosa* community biofilms as a tool to study interactions between microbial colonies, with regards to spatial distribution, biofilm integration and formation of biofilm components.

2. Materials and methods

2.1. Microorganisms and culture media

Pseudomonas aeruginosa PAO1 and *Komagataeibacter hansenii* (ATCC 53582) strains were used as matrix builders. *Pseudomonas* strain was cultured in standard LB medium (Thermo Fisher Scientific). To culture *Komagataeibacter,* standard Hestrin-Schramm (HS) medium containing 2 % glucose, 0.5 % bacterial peptone, 0.5 % yeast extract, 0.27 % sodium phosphate dibasic and 0.115 % citric acid with pH 5.5 was used [23]. Respective medium was inoculated with a loopful of growing stock culture and the culture was grown on a rotary shaker (200 rpm) at suitable conditions overnight.

2.1.1. Production of BC

Sterile HS medium in a 6-well plate was inoculated with 5 % (v/v) *K. hansenii* overnight culture. The inoculated plates were incubated at 26 ± 1 °C in stationary condition for 5 days to allow for BC biofilm matrix production.

2.1.2. Media compatibility for co-culturing

K. hansenii and *P. aeruginosa* overnight-grown cultures (diluted to 0.1 OD at 600 nm) were inoculated into LB, HS and LB + HS (1:1) media at 5 % (v/v) inoculum. Cell density was measured every 15 min at 600 nm (Tecan microplate reader) for 15 h to check the growth pattern and medium compatibility.

2.1.3. Co-culture conditions

Co-culturing was performed in two ways by introducing overnight grown cultures or preformed BC matrix. In the first method, *K. hansenii* and *P. aeruginosa* were co-cultured in HS medium at various ratios (1:1 to 10:1). Higher *K. hansenii* inoculum was used due to its longer doubling time (8–10 h) compared to *P. aeruginosa* (30–50 min). In the second method, *P. aeruginosa* was co-cultured with 5-day BC biofilm matrix (pellicle) produced by *K. hansenii*. The co-cultures were incubated at 26 °C for 5 days at stationary condition. *K. hansenii* monoculture served as control along with the resulted BC for further characterization. Control BC and co-culture biofilm in HS at 26 °C and *P. aeruginosa* monoculture biofilm in LB media at 37 °C were produced.

2.1.4. Purification

Two sets of co-cultured biofilms were harvested by removing them from the liquid-air interface. One set of biofilms were treated with 1 % NaOH for 15 min to remove cells and other media impurities embedded in the biofilm and rinsed thoroughly with water until a neutral pH was attained in the drained water. The other set of biofilms were left untreated to investigate the effect of co-culture and integration of biofilms. The biofilms were freeze-dried and stored in a desiccator for further analyses.

2.2. Characterization of co-cultured biofilm

The surface morphology and structural integration of co-cultured biofilm was imaged by field emission scanning electron microscope (JEOL, JSM-6700 F). The scanning electron microscope was operating at an accelerating voltage of 1.5 V. The freeze-dried biofilm samples were mounted on stubs by sticking with double sided carbon tape, sputter coated with platinum for 70 s at 20 mA current in vacuum condition. The coated samples were used for imaging at different magnifications as required.

The change in the crystallinity of co-cultured biofilms were determined by X-ray diffraction (XRD) using Bruker portable X-ray diffractometer (Rigaku) with Cu tube radiation generated at 30 kV voltage and

10 mA current. The freeze-dried biofilms were pressed and mounted onto a quartz sample holder. The data were generated in reflection mode and collected in the 2θ range of 5–70° with a step size of 0.026°. Thermogravimetric analyzer (TGA Q50, TA Instruments) was employed to measure the amount and rate of change in weight of the co-culture biofilms, either as a function of increasing temperature or time, in a controlled atmosphere. The sample (2–5 mg) was kept in an alumina crucible, heated in the furnace, and flushed with N_2 gas at the rate of 40 ml/min, from 30 to 800 °C, at the rate of 10 °C/min [24]. The percentage weight loss was plotted against temperature. Result was analyzed using TA Universal 2000 software. Swelling ability and moisture content were determined by immersing freeze dried co-cultured biofilms in 8 ml water at room temperature for 4 h. The initial and swollen film weights were used to calculate swelling ratio, swelling percentage, and moisture content. Rheological measurement was conducted using Haake Mars rheometer (Thermo Fisher Scientific). Parallel plate geometry with plate diameter of 15 mm was used. Gap was set at 1.5 mm and strain percentage was set to 1 %. Steady shear tests were conducted between 1 and 100 Hz in frequency sweeps. Three replicate scans were observed, wherein storage modulus (G′), loss modulus (G″) were recorded. The viscoelasticity (tan δ) was calculated using G”/G’. The changes in the viscoelastic properties of co-cultured biofilms were analyzed [21].

FTIR spectra of co-cultured biofilms were obtained by using ATR spectrophotometer (PerkinElmer). All measurements were carried out at room temperature in anhydrous conditions with air as the background. For each sample, 32 scans at a 4 cm^{-1} resolution were collected in the range of 4000–450 cm^{-1}.

Confocal laser scanning microscope (Zeiss LSM 710 META) system was used to image co-cultured biofilms with a 20x objective lens. To examine the extent of *P. aeruginosa* PAO1 infiltration into BC matrix, the spatial distribution of microbes and EPS/eDNA development, was assessed. For this experiment *P. aeruginosa* and *K. hansenii* cultures tagged with YFP and RFP respectively were used. SYTO^{TM}9, propidium iodide stains for live dead microbial assay (viability and distribution of microbial cells) and TOTO^{TM}-1 (Green) extracellular nucleic acid stain (eDNA staining and average microbial ratio count) were used for imaging the co-cultured biofilms. The dyes were excited by Argon ion laser at wavelengths recommended by the manufacturers.

Tensile strength (TS) and percent elongation (%E) at break of BC control and cocultured biofilms (press and freeze dried) were measured as per ASTM D 882/1995 using Instron 5567 electromechanical tester with 50 N load cell and tensile extension of 3 mm/min. TS was calculated by dividing the maximum load for breaking the film by cross-sectional area and %E by dividing film elongation at rupture to initial gauge length at an ambient temperature (25 ± 2 °C). The reported values are average of 8*3 measurements.

The significant difference between BC control and co-cultured BC matrix grown with *P. aeruginosa* [BC(PA01)] was evaluated by Student’s t-test (<0.05) in OriginPro V2022b software.

3. Results

3.1. Pseudomonas aeruginosa PAO1 cells colonize the surface and the interior of Komagataeibacter hansenii biofilm

The growth and penetration of *P. aeruginosa* PAO1 into the BC matrix was demonstrated through surface morphology analysis following co-culturing of *K. hansenii* with *P. aeruginosa* PAO1 in HS medium. HS medium is the optimized medium for *K. hansenii* to grow and produce BC pellicles [25], while LB has been demonstrated as a medium for *P. aeruginosa* pellicle growth. Culturing *K. hansenii* in LB showed no observable growth (Fig. S1A), while culturing *P. aeruginosa* in HS medium under conditions optimum for *K. hansenii* (pH 5 at 26 °C) revealed growth (Fig. S1B). Co-culturing of *K. hansenii* and *P. aeruginosa* PAO1 in HS, resulted in no BC matrix production (BC pellicle formation at the air-liquid interface, Fig. S2) when inoculated with ratios of 1:1 to 10:1 [23,26]. Thus, inoculation of *P. aeruginosa* with pre-cultured biofilms of *K. hansenii* were subsequently used to study the effect of pre-existing matrix on eDNA by *P. aeruginosa*.

Untreated BC harvested from monocluture shows uniform distribution of *K. hansenii* in its native matrix (Fig. 1A). Similarly, in the hybrid BC matrix BC(PAO1) resulting from the co-culturing of BC with *P. aeruginosa*, bacterial cells are uniformly distributed across the surface of the biofilm (Fig. 1B). The lower resolution of Fig. 1b compared to Fig. 1a could indicate the deposition of EPS on BC fibers and bacterial cells.

Washing the BC and BC(PAO1) biofilms removed bacterial cells without affecting matrix integration (Fig. 2). *K. hansenii* monoculture biofilms consisting of BC (referred to as BC control), contained randomly arranged, nano-porous, nano-fibrous network structures (Fig. 2a). Following inoculation with *P. aeruginosa* BC(PAO1), these nanopores were occupied, at least superficially, by an additional material that is suspected to be *P. aeruginosa* matrix (Fig. 2b), which provides evidence of integration of *P. aeruginosa* biofilm (EPS) into the BC matrix.

3.2. Physicochemical changes to the matrix upon co-culturing indicate colonization of K. hansenii biofilm by P. aeruginosa

BC matrix is highly crystalline in nature. In our study, integration of *P. aeruginosa* PAO1 biofilm to the BC matrix changes the degree of crystallinity. Understanding crystallinity is significant as it affects the physical properties such as storage modulus, permeability, density and melting temperature. The X-ray diffraction (XRD) results of BC control and BC(PAO1) show typical diffraction peaks (2θ) at 14.75°, 16.41° and 22.75°, assigned to the cellulose-I crystalline form [27] indicating high crystallinity (Fig. 3). However, the decrease in peak intensity at 2θ = 14.75° for BC(PAO1) suggests that the crystallinity of the co-cultured biofilms is lower compared to the BC control (Fig. 3A). Interestingly, without NaOH treatment, no significant changes were observed for BC and BC(PAO1) which may be attributed to the presence of media components, bacterial cells, and metabolites (Fig. 3B).

To understand the thermal decomposition behavior of BC control and co-cultured BC(PAO1), thermogravimetric analysis (TGA) was performed. TGA provides understanding of weight changes on heating and the phase changes due to decomposition and oxidation. The thermal decomposition behaviors depend on, for example, heating rate, mass and sample geometry. The TGA curve is obtained by plotting percent weight loss against temperature. The maximum weight loss observed in NaOH-treated and untreated BC control was 99 and 92 %, respectively (Fig. 4A & C). Interestingly, for BC(PAO1) the weight loss was only up to 70 % (Table 1). The differential thermal gravity (DTG) shows that the endothermic peaks are attenuated following PAO1 colonization, as indicated for the NaOH-treated BC and BC(PAO1) samples by an attenuation of the 337 °C degradation peak (Fig. 4B), and for the untreated samples at 308 °C (Fig. 4D).

BC is well-known for its unique water retaining characteristic due to nanofibrous, highly porous, 3D structure. It is evident from the SEM images that EPS integration has affected the porosity of the BC matrix. To support this information, swelling ratio and moisture content of the co-cultured biofilms and BC control were recorded (Table 2). There is significant reduction in swelling ratio and moisture content of BC(PAO1) compared to BC control, as expected.

3.3. P. aeruginosa PAO1 produces EPS within scaffold that interacts with cellulose

Attenuated total reflectance (ATR) spectral analysis was performed to determine the extent to which the composition of the biofilm matrix was modified by co-culturing. The ATR spectra of BC control and co-cultured BC(PAO1) biofilms, with and without NaOH treatment are shown in Fig. 5. All biofilms exhibited characteristic cellulose vibration

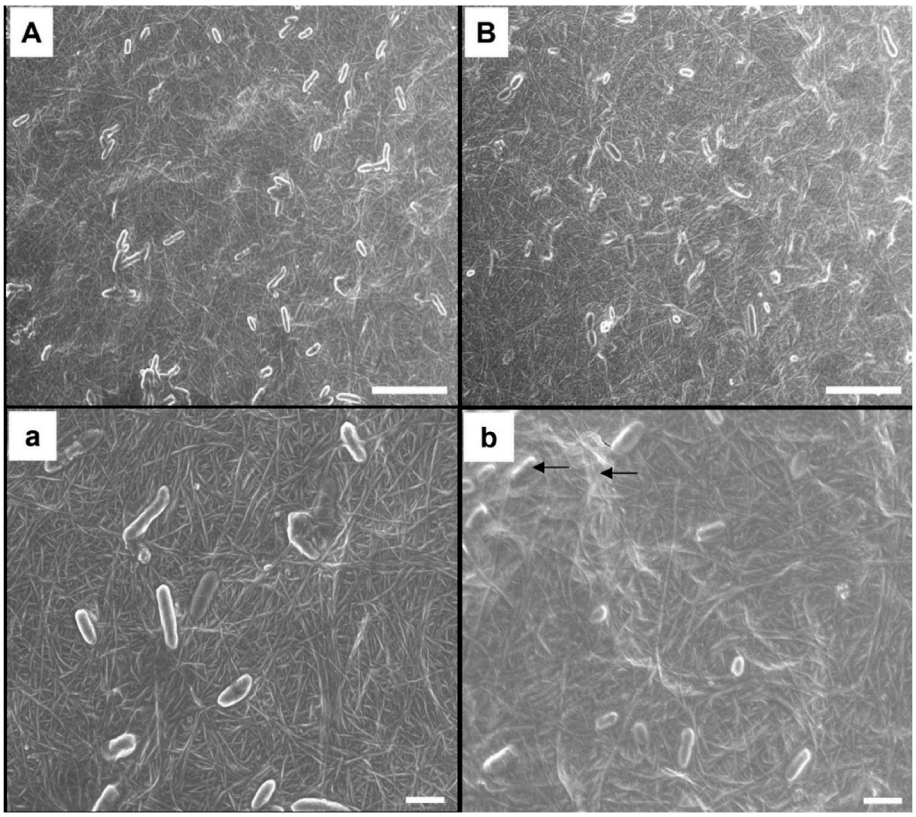

Fig. 1. Scanning Electron Microscopy (SEM) images of biofilms visualized with 2K (A&B, Scale – 10 μm) and 5K (a&b, Scale – 10 μm) magnification for (A, a) BC from *K. hansenii* and (B, b) BC co-cultured with *P. aeruginosa* PAO1. Black arrow indicates EPS deposition on BC fibers and bacterial cells.

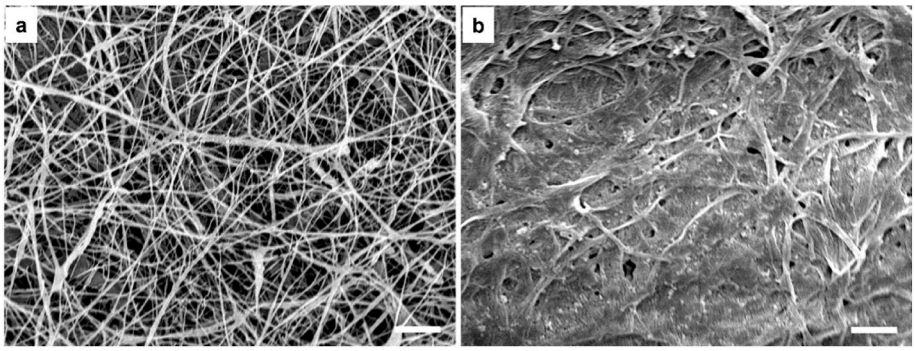

Fig. 2. SEM images of biofilms treated with NaOH at 12K (Scale – 1 μm) magnification. (a) BC control from *K. hansenii* monoculture (b) BC co-cultured with *P. aeruginosa* PAO1.

peaks. In the co-cultured biofilms, there was reduction in peak intensities at 2900, 1500 to 899 cm^{-1} that are characteristic of amorphous cellulose. The peak at 1643 cm^{-1} indicates water bound O–H groups of cellulose [28]. The broad bands between 3650 and 3000 cm^{-1} correspond to O–H stretching vibrations which was related to hydrogen bonding in the cellulose network. The broadened absorption peak near 3400 cm^{-1} belongs to O–H groups and water [29]. Attenuation of these bands in the co-cultured biofilms, suggests that EPS secreted following PAO1 colonization have formed H-bonds with the cellulose O–H groups, thereby aggregating the cellulose microfibrils [30]. The absence of significant 1240, 1075 cm^{-1} PO_2 stretching DNA peaks indicate a low concentration of eDNA in the co-cultured biofilm compared to cellulose [31].

3.4. eDNA is not expressed by P. aeruginosa in or on the K. hansenii biofilm following onset of colonization

Confocal microscopy analyses of 19 μm thick Z-stack of BC(PAO1) show that both populations are present throughout the BC biofilm (Fig. 6A). *P. aeruginosa* can infiltrate the BC matrix following inoculation, as indicated by the even distribution of *P. aeruginosa* (YFP-tagged, green) and *K. hansenii* (RFP-tagged, red) cells throughout the BC matrix on day 4 (Fig. 6A). While TOTO-1-stained *P. aeruginosa* PAO1 biofilm (Fig. 6B) showed eDNA streaks throughout, no traces of eDNA were observed within the folds of cellulose fibres of *K. hansenii* BC biofilm (Fig. 6C). The low intensity fluorescent signals from TOTO-1 persist in *K. hansenii* biofilms even after DNaseI treatment, which indicates that the signal arises due to autofluorescence of cellulose fibres and eDNA is not present in *K. hansenii* (Fig. S5). The fluorescence property of cellulose in the range of 550 nm is attributed to glycosidic bonds between the

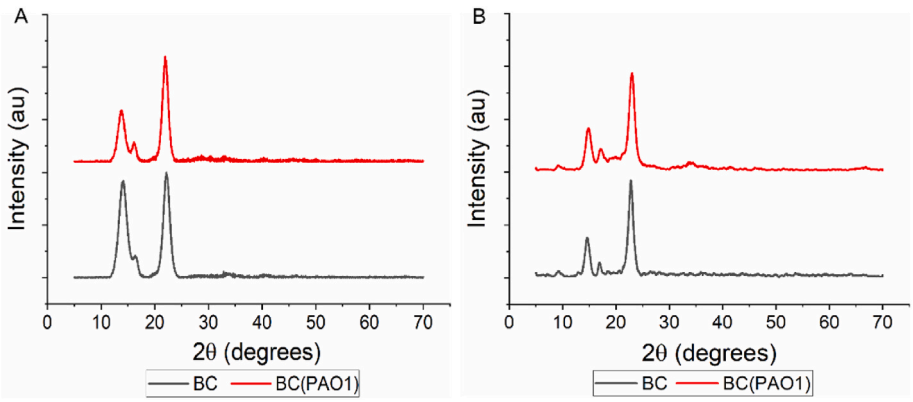

Fig. 3. XRD patterns of biofilms - BC from *K. hansenii*, BC co-cultured with *P. aeruginosa* PAO1, n = 3. (A) with NaOH and (B) without NaOH treatment.

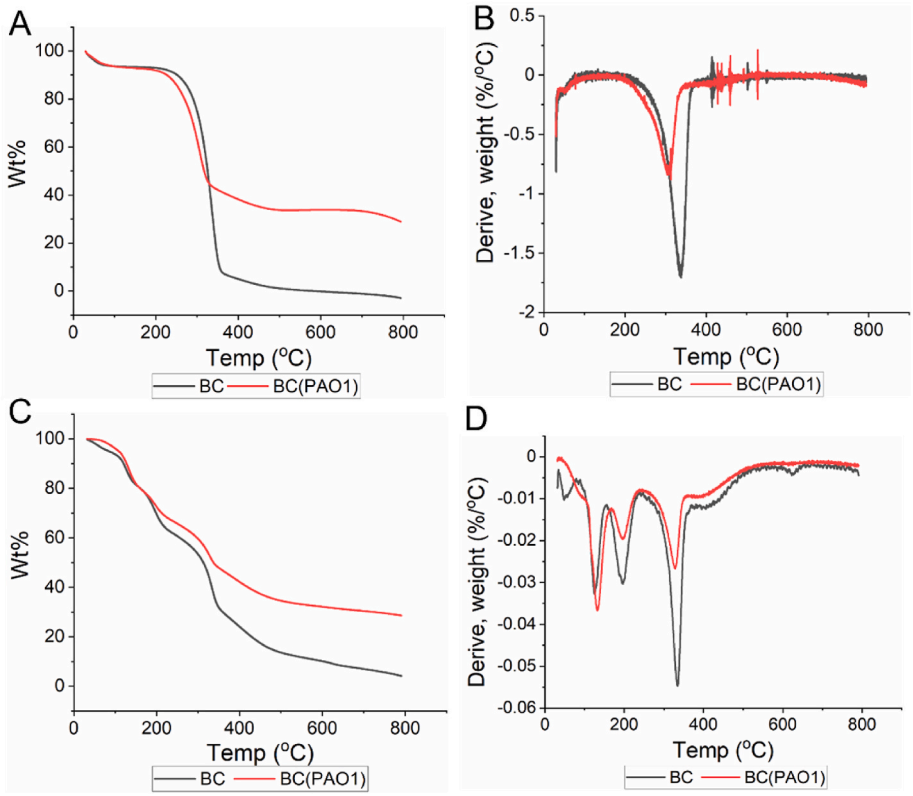

Fig. 4. TGA and DTG thermograms of biofilms - BC from *K. hansenii*, BC co-cultured with *P.* PAO1, n = 3. TGA thermograms of the biofilms (A) with and (C) without NaOH treatment and DTG thermograms of the the biofilms (B) with and (D) without NaOH treament.

Table 1
Thermal Properties of biofilms with and (without) NaOH treatment (n = 3; Decomposition Wt% - t statistic = 23.06, DF = 1, p = 0.027; Max. Wt% loss - t statistic = 11.13, DF = 1, p = 0.049). At 0.05 confidence interval, thermal properties of BC(PAO1) is significantly different from BC control.

Sample	Decomposition (T_{max})		Maximum loss	
	Wt (%)	Temp (°C)	Wt (%)	Temp (°C)
BC	90.69 ± 2.07 (67.04 ± 4.13)	355.77 ± 30.18 (345.95 ± 15.34)	98.91 ± 2.12 (91.47 ± 3.75)	500.02 ± 32.97 (638.47 ± 31.42)
BC(PAO1)	55.35 ± 3.86 (50.58 ± 2.84)	329.4 ± 24.88 (339.85 ± 29.02)	66.27 ± 3.10 (68.87 ± 5.28)	497.85 ± 20.16 (652.11 ± 41.09)

*Number in Parentheses represents thermal stability of biofilms without NaOH treatment.

glucose molecules [32]. Images of co-cultured biofilm on day 5 stained with SYTO 9 and propidium iodide were taken at 4, 9 and 17 μm thickness (same location). This showed a higher distribution of SYTO 9-stained green viable bacterial cells throughout the matrix compared to dead cells (red). There was higher distribution of cells at the top (close to surface at 4 μm slice) (Fig. 6D) and a sparse distribution in the in-between section of 9 μm slice (Fig. 6E). Bacterial cell concentrations is increased significantly with depth 17 μm (Fig. 6F) of the BC matrix up to the imaging limit (17-19 μm).

Confocal images were taken at different timepoints stained with

Table 2
Swelling ability and moisture content of biofilms with and (without) NaOH treatment (n = 3; Swelling % - t statistic = 11.12, DF = 9, $p < 0.0001$; Moisture % - t statistic = 161.95, DF = 3, $p < 0.0001$). At 0.05 confidence interval, the swelling ratio and moisture % of BC(PAO1) is significantly different from BC control.

Sample	Swelling ratio*	Swelling ratio (%)*	Moisture content (%)*
BC	44.98 ± 6.10 (35.77 ± 5.59)	4498 ± 610.69 (3577 ± 559.68)	97.79 ± 0.29 (92.34 ± 1.42)
BC(PAO1)	29.00 ± 7.21 (28.21 ± 7.45)	2900 ± 721.67 (2821 ± 745.86)	96.51 ± 0.81 (89.93 ± 0.97)

*Numbers in parentheses represent swelling ability and moisture content of biofilms without NaOH treatment.

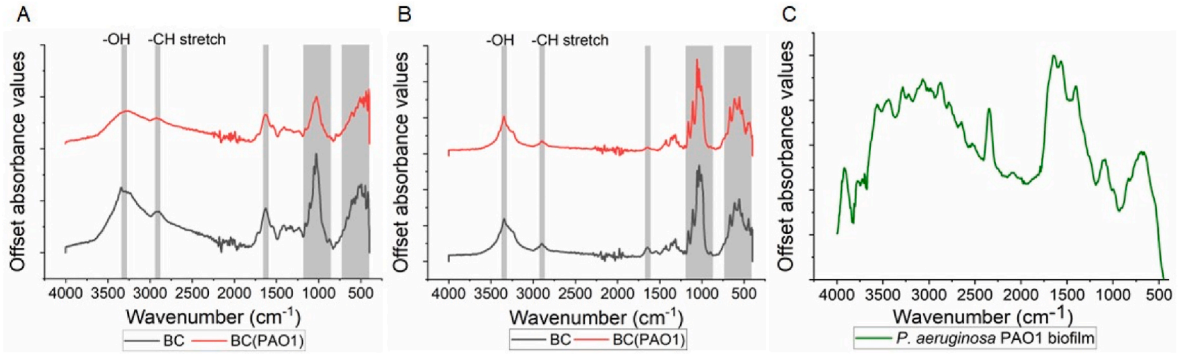

Fig. 5. FTIR-ATR spectra of BC from *K. hansenii* monoculture and BC co-cultured with *P. aeruginosa* PAO1, n = 3. (A) NaOH-treated biofilms, (B) untreated biofilms, (C) *P. aeruginosa* PAO1 monoculture biofilm. Gray blocks represent characteristics cellulose vibration peaks.

TOTO-1 (day 2, 3 and 5) indicate biofilm formation by infiltration of YFP-tagged *P. aeruginosa* cells into the BC matrix with RFP-tagged *K. hansenii*. The results were consistent with the biophysical characterization showing matrix integration. The abundance of eDNA fibres on the surface of co-cultured biofilm decreased over time and by day 5 it was absent altogether, despite the fact that PAO1 cells were present in high numbers (Fig. 6G–I). The average bacterial counts for *P. aeruginosa* PAO1 and *K. hansenii* across all depths on day 5 of biofilm (Fig. 6I) growth were 67 ± 4 % and 33 ± 6 %, respectively (n = 10*3). The depletion of eDNA fibres suggests that colonization on preformed matrix might inhibit eDNA production by *P. aeruginosa*, where eDNA fibres were absent in the matrix on day 5, which was in contrast to the day 5 *P. aeruginosa* monoculture biofilm (Fig. 6B and C). However, additional interpretation is that the eDNA is not retained by the biofilm matrix or that a DNase that degrades the eDNA under these co-culturing conditions. Many pathogens produce extracellular DNase and eDNA degradation might be from *Pseudomonas* sp. as there is no requirement for eDNA due to presence of preformed matrix [33]. There are no reports that *K. hansenii* secretes DNase. Given that the system is static and there is eDNA around at day 2 that disappears at day 5, eDNA is being actively degraded in this co-culture. Repeating this study on matrices with different chemical composition and porosity could inform a critical mesh size for inhibiting eDNA production. Currently, however, controlling physicochemical properties to the extent required to conduct this experiment would not be possible.

3.5. *P. aeruginosa* colonization shows no change in mechanical properties of *K. hansenii* biofilm

Integration of EPS into preformed matrix would be expected to modulate rheological properties. Tan δ is slightly lower for BC(PAO1) than BC following NaOH treatment of both (Fig. 7A). These results indicate that the storage modulus (i.e., elasticity) relative to the loss modulus (i.e., viscosity) is increased. However, without NaOH treatment, no significant changes in the rheology of the matrix are observed (Fig. 7B).

To further illustrate the effect of *P. aeruginosa* colonization on the mechanical properties of BC nanofibers, Fig. 8 shows the mean value and standard deviation of tensile strength at break, Young's modulus, and elongation at break. No significant changes are observed with co-cultured biofilms suggesting that the interaction of *P. aeruginosa* EPS with BC fibers does not significantly impact the mechanical strength of BC matrix. This could indicate further that *P. aeruginosa* has not synthesized eDNA, as eDNA was shown previously to promote the formation of the viscoelastic extracellular network structure in the same *P. aeruginosa* model biofilm system [21].

4. Discussions

To date, eDNA is understood to be released as a consequence of autolysis in biofilm systems [18]. The released eDNA has been shown to provide structural scaffold and mechanical resistance to biofilms by forming extracellular matrix [20]. However, in this study, we suggest that eDNA release is an active cell regulated mechanism. This is due to the attenuation of eDNA production after day 3 in the presence of preformed BC matrix of our co-cultured *in vitro* model of PAO1 and *Komagataeibacter* sp. One reason for this observation might be due to the highly nanofibrous structures of cellulose (Fig. 2) which provide optimal surface for efficient cell adsorption. Additionally, higher moisture content along with nanoporous structures of cellulose provide favourable nutrient rich conditions for PAO1 growth without the need for eDNA production during the later stages of biofilm formation.

Our study reports the development of a reproducible polymicrobial biofilms model that is intended to be used for understanding the co-existence, interaction, structural integration, biofilm components modification and relationships between mixed microbial population that exist in nature. The model is developed by using preformed BC from *K. hansenii* 53582 instead of co-culturing the two as we experienced that *P. aeruginosa* outgrows *K. hansenii* 53582, likely due to shorter doubling time (30–50 min compared to 8–10 h) or the production by *P. aeruginosa* of metabolites that inhibit competitors (e.g., pyocyanin). There was no sign of BC matrix production even with increased inoculum ratios of *K. hansenii*.

The microscopy results of co-cultured biofilm, BC(PAO1), clearly indicate biofilm integration as suggested by the significantly denser, heterogeneous surface, less porous with larger ribbons coated with EPS and infiltration of *P. aeruginosa* PAO1 into the BC matrix. These results are in agreement with earlier reports, as EPS plays a significant role in regulating the bundling process of BC microfibrils, resulting in larger bundles. The bundling of nanofibers was promoted by coating co-

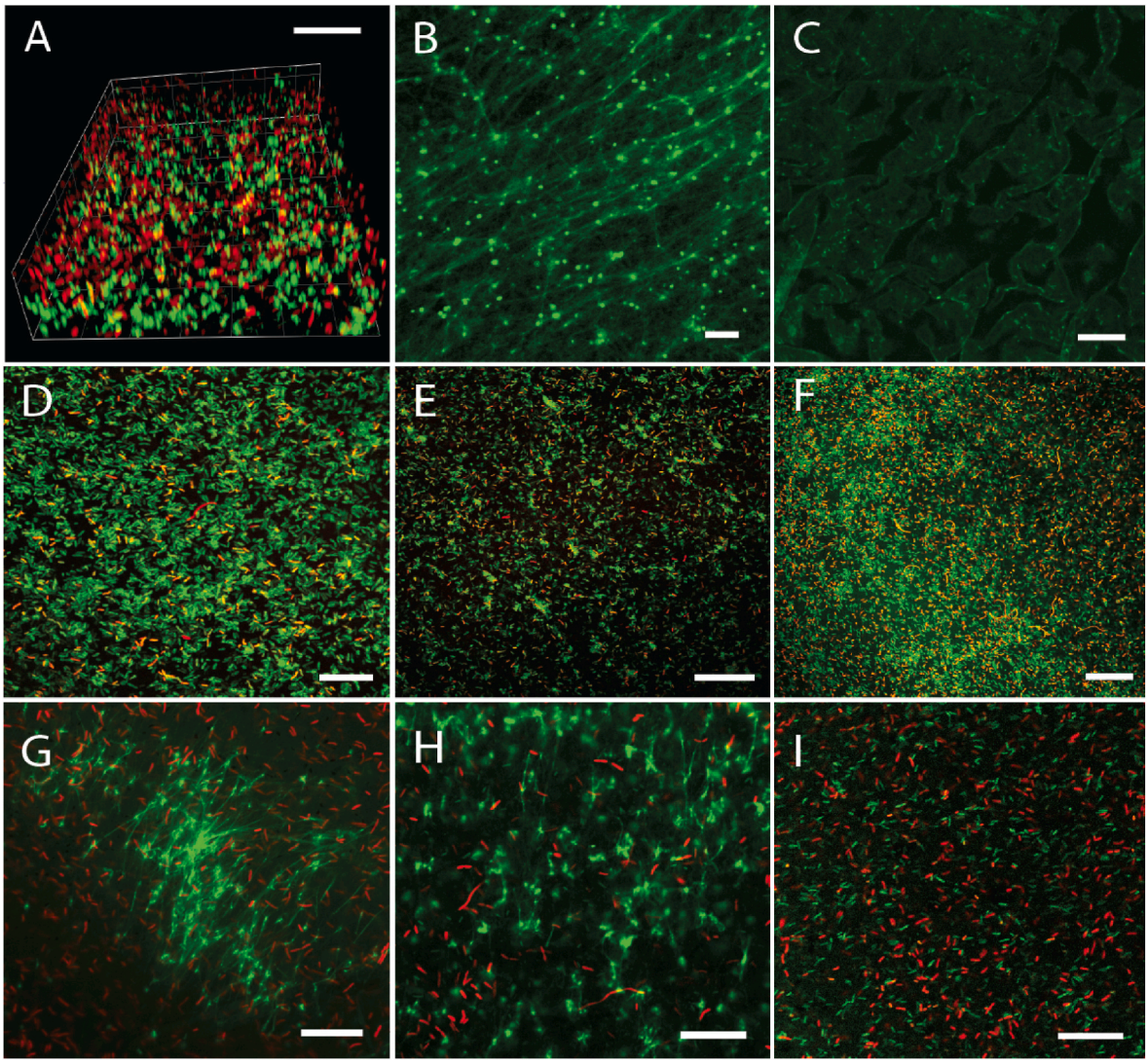

Fig. 6. Confocal images of biofilm. Green - YFP-*Pseudomonas aeruginosa* PAO1; Red - RFP-*Komagataeibacter hansenii* 53582; Yellow = green + red - RFP-*Komagataeibacter hansenii* 53582. (A) Composition and abundance of microbes in co-cultured biofilm across 19 μm-thick biofilm (day 4). (B) Monoculture *P. aeruginosa* PAO1 biofilm (day 5) showing eDNA at depth of 3 μm from the biofilm-medium interface. (C) Monoculture *K. hansenii* BC biofilm (day 5) at a depth of 3 μm from the biofilm-medium interface. (D,E,F) Co-cultured biofilms stained with SYTO 9 (green) and propidium iodide (red) a nucleic acid stain (day 5) showing infiltration of *P. aeruginosa* PAO1 into BC matrix at 4, 9 and 17 μm thickness, respectively. (G,H,I) Co-cultured biofilms at day 2, 3 and 5 stained with TOTO-1 (green) eDNA stain. All three images were at 3rd μm of 18 μM thick biofilm. BC co-cultured with *P. aeruginosa* PAO1 biofilm showing uniform distribution of bacterial cells with green eDNA fibres (day 2) and absence of eDNA at day 5 (Scale – 10 μm). (For interpretation of the references to colour in this figure legend, the reader is referred to the Web version of this article.)

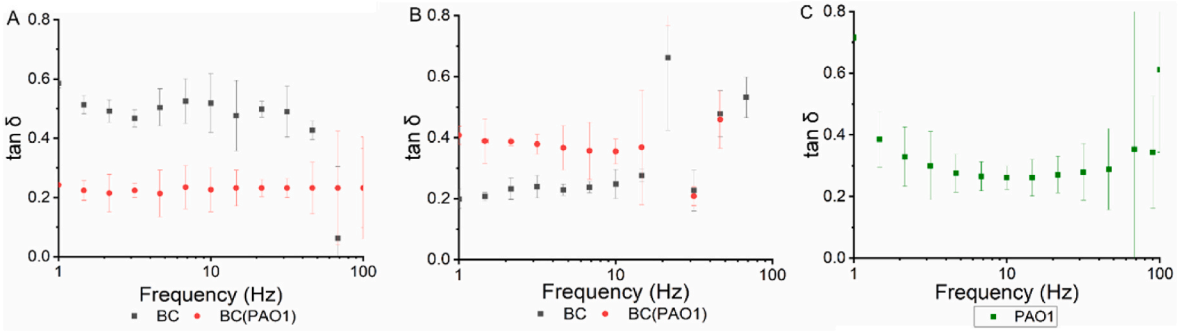

Fig. 7. Visco-elasticity of biofilms - BC from *K. hansenii*, BC co-cultured with *P. aeruginosa* PAO1. (A) Biofilms with NaOH treatement, (B) biofilm without NaOH treatement, (C) *P. aeruginosa* PAO1 monoculture biofilm. Tan δ, increased storage modulus (i.e., elasticity) relative to the loss modulus (i.e., viscosity) in BC(PAO1) compared to BC control (n = 3; t statistic = 1.77, DF = 13, p = 0.099). At 0.05 confidence interval, the viscoelasticity of BC(PAO1) is not significantly different from BC control.

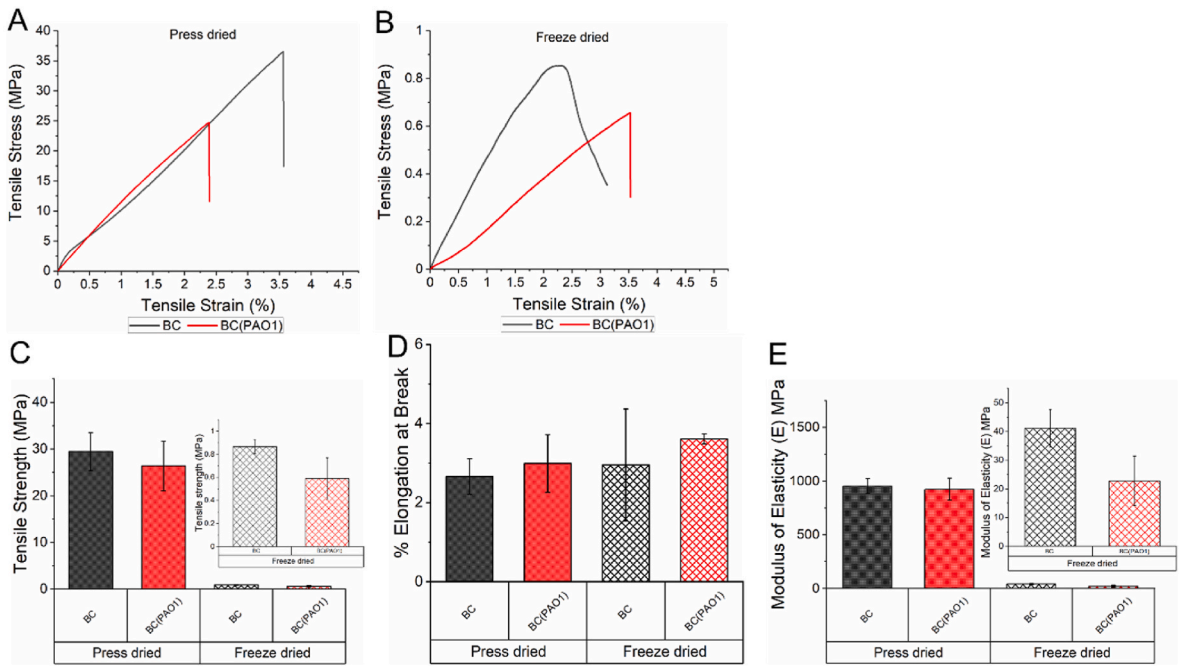

Fig. 8. Mechanical characterizations of co-cultured biofilms processed by press drying and freeze drying, treated with NaOH – BC control, BC co-cultured with *P. aeruginosa* PAO1. (A) Tensile strength of press dried films, (B) Tensile strength of freeze-dried films, (C) Tensile strength at break, inset shows low tensile strength, (D) Percentage elongation at break ϵ Modulus of Elasticity, inset shows low elasticity (n = 8*3; Tensile strength - t statistic = 1.09, DF = 5, p = 0.32; Elongation at break - t statistic = 1.07, DF = 5, p = 0.33); Young's modulus - t statistic = 1.07, DF = 5, p = 0.35. At 0.05 confidence interval, the mechanical properties of BC(PAO1) are not significantly different from BC control.

crystallized microfibrils. Aggregation of co-crystallized microfibrils is due to van de Waals interactions and hydrogen bond [30,34]. Bacterial motility facilitates interaction by penetration into the existing biofilm promotes colonization by invasion into the fibres. *P. aeruginosa* preferential growth on BC matrix might be due to depletion of oxygen and limited nutrients. Growing within the biofilm is advantageous for growth and survival of any organism, but favourable rich environment suppressing the release of eDNA foundation matrix cannot be considered. It is reported that biofilms with eDNA presence in bacterial infected wounds are difficult to treat and heal [35].

It is evident that *P. aeruginosa* outcompetes *K. hansenii.* The nonappearance of eDNA at the end of co-culturing strongly indicates that *P. aeruginosa* PAO1 can modify its strategy for biofilm assembly when a structural scaffold is already available, as illustrated here with a preformed BC matrix along with viable *K. hansenii* cells.

The changes in the physicochemical properties of co-cultured BC (PAO1) in comparison to BC control indicate that PAO1 EPS is interacting with BC nanofibers. The XRD results show a reduction in crystallinity of co-cultured biofilm which could be due to the amorphous nature of EPS [36]. Insertion of polymeric material into the existing crystalline biopolymer has been reported to cause crystallinity reduction [37,38]. The incorporation and penetration of EPS molecules with the cellulose microfibrils disrupts the original hydrogen–bonding interactions between the cellulose microcrystalline chains [37]. Tensile testing of co-cultured BC(PAO1) revealed no significant changes in the Young's modulus, stress at break, and strain at break compared with BC control. While improved mechanical strength was expected, the high concentrations of EPS, coating the surface of co-crystallised microfibrils might have disrupted their additional aggregation and networking with bacterial cellulose microfibrils. Hence, impeding enhancement of its mechanical strength [30,39]. However, in the absence of eDNA, which is known to dominate the elasticity of *P. aeruginosa* biofilms, the mechanical properties and strcutural integrity of BC remain unaffected by EPS from *P. aeruginosa*. Prior studies have shown similar results. There was no significant change in the mechanical properties by co-culturing *K. hansenii* ATCC 23769 with *E. coli* ATCC 35860, which produces a high concentration of EPS (41.4 mg/ml), but had a significant increased mechanical strength by co-culturing with *E. coli* ATCC 700728, which produces relatively low concentration (3.4 mg/ml) of EPS [30].

The TGA results revealed that the initial weight loss below 200 °C was due to dehydration and at higher temperature the cleavage of glycosidic bonds occurs with rapid weight loss. The maximum weight loss is related to pyrolysis of the β-1,4-glycosidic bond [24]. The less intense and wider endothermic peaks corresponding to reduced crystallinity and increased thermal stability of BC(PAO1) co-cultured biofilm. The addition of EPS is likely to cause disruption of the regular arrangement among the glucose molecules. The TGA results on BC (PAO1) are consistent with the XRD results and further confirm the integration of EPS (increased amorphous content) into BC matrix as reflected by the extended degradation temperature, thermal stability and reduced crystallinity of the co-cultured biofilm. The substantial reduction in swelling ratio and moisture content of BC(PAO1) can be attributed to reduced porosity of BC matrix compared to BC control, caused by EPS coating over BC nanofibers.

5. Conclusion

Co-culturing a preformed BC matrix of *K. hansenii* with *P. aeruginosa* PAO1 resulted in integration of the two populations. This is demonstrated by complete distribution of cells over BC matrix, significantly denser more heterogeneous surface, and a less porous structure with thick bundled fibres coated with EPS. Extended degradation temperature, improved thermal stability and reduction in crystallinity, swelling ratio and moisture content of the co-cultured biofilm in comparison to BC control, further indicate colonization of *K. hansenii* BC matrix by *P. aeruginosa*. The co-culturing method using a preformed matrix is an innovative approach to design and test interactions between the species. FTIR and confocal images indicates the absence of eDNA in the co-cultured biofilms after day 3, and that when a preformed matrix exists, *P. aeruginosa* does not produce eDNA. Further research is required to

understand the critical limits for inhibiting eDNA production by *P. aeruginosa* in various preformed matrix environment (with regards to e.g., viscoelasticity and mesh size).

Funding

This work was partially supported by the National Research Foundation, Singapore, under its Competitive Research Programme (Award # NRF-CRP22-2019-0005) and Agency for Science, Technology and Research Additive Manufacturing for Biological Material (AMBM) programme (A*STAR Grant # A18A8b0059).

CRediT authorship contribution statement

Usha Rani Mahadevaswamy: Conceptualization, Data curation, Formal analysis, Investigation, Methodology, Resources, Software, Validation, Writing – original draft, Writing – review & editing. **Sudarsan Mugunthan:** Conceptualization, Data curation, Investigation, Methodology, Validation, Data curation, Formal analysis, Investigation, Methodology, Software, Validation. **Thomas Seviour:** Conceptualization, Formal analysis, Investigation, Methodology, Supervision, Validation, Writing – review & editing. **Staffan Kjelleberg:** Conceptualization, Funding acquisition, Investigation, Supervision, Validation, Visualization, Writing – review & editing. **Sierin Lim:** Conceptualization, Funding acquisition, Project administration, Supervision, Writing – review & editing, Validation, Visualization.

Declaration of competing interest

Authors have no competing interests in this study.

Data availability

The complete dataset will be made available upon request and can be accessed through this link: https://doi.org/10.21979/N9/MGU6KY

Acknowledgement

The authors thank Scott Rice at Singapore Center for Environmental Life Sciences Engineering (SCELSE) for technical discussion on the imaging of co-cultured biofilm.

Appendix A. Supplementary data

Supplementary data to this article can be found online at https://doi.org/10.1016/j.bioflm.2024.100176.

References

[1] Flemming HC, Wingender J. The biofilm matrix. Nat Rev Microbiol 2010;8:623–33. https://doi.org/10.1038/nrmicro2415.
[2] Gloag ES, Fabbri S, Wozniak DJ, Stoodley P. Biofilm mechanics: implications in infection and survival. Biofilms 2020;2:100017. https://doi.org/10.1016/j.bioflm.2019.100017.
[3] Flemming HC, Neu TR, Wozniak DJ. The EPS matrix: the "house of biofilm cells". J Bacteriol 2007;189:7945–7. https://doi.org/10.1128/jb.00858-07.
[4] Flemming HC, Wingender J, Szewzyk U, Steinberg P, Rice SA, Kjelleberg S. Biofilms: an emergent form of bacterial life. Nat Rev Microbiol 2016;14:563–75. https://doi.org/10.1038/nrmicro.2016.94.
[5] Tran Thi MT, Wibowo D, Bernd Rehm HA. *Pseudomonas aeruginosa* biofilms. Int J Mol Sci 2020;21:8671. https://doi.org/10.3390/ijms21228671.
[6] Periasamy S, Nair HAS, Lee KWK, Ong J, Goh JQJ, Kjelleberg S, Rice SA. *Pseudomonas aeruginosa* PAO1 exopolysaccharides are important for mixed species biofilm community development and stress tolerance. Front Microbiol 2015;6:851. https://doi.org/10.3389/fmicb.2015.00851.
[7] Karygianni L, Ren Z, Koo H, Thurnheer T. Biofilm Matrixome: extracellular components in structured microbial communities. Trends Microbiol 2020;28:668–81. https://doi.org/10.1016/j.tim.2020.03.016.
[8] Reichhardt C, Parsek MR. Confocal laser scanning microscopy for analysis of *Pseudomonas aeruginosa* biofilm architecture and matrix localization. Front Microbiol 2019;10. https://doi.org/10.3389/fmicb.2019.00677.
[9] Bowen WH, Burne RA, Wu H, Koo H. Oral Biofilms: pathogens, matrix, and polymicrobial interactions in microenvironments. Trends Microbiol 2018;26:229–42. https://doi.org/10.1016/j.tim.2017.09.008.
[10] Ramírez Granillo A, Sanchez Espindola ME, Martínez Rivera MA, Bautista de Lucio VM, Rodríguez Tovar AV. Antibiosis interaction of *Staphylococccus aureus* on *Aspergillus fumigatus* assessed in vitro by mixed biofilm formation. BMC Microbiol 2015;15(33):1–15. https://doi.org/10.1186/s12866-015-0363-2.
[11] Fourie R, Pohl CH. Beyond antagonism: the interaction between *Candida* species and *Pseudomonas aeruginosa*. J Fungi (Basel) 2019;5. https://doi.org/10.3390/jof5020034.
[12] Freilich S, Zarecki R, Eilam O, Segal ES, Henry CS, Kupiec M, Gophna U, Sharan R, Ruppin E. Competitive and cooperative metabolic interactions in bacterial communities. Nat Commun 2011;2:589. https://doi.org/10.1038/ncomms1597.
[13] Seto A, Saito Y, Matsushige M, Kobayashi H, Sasaki Y, Tonouchi N, Tsuchida T, Yoshinaga F, Ueda K, Beppu T. Effective cellulose production by a coculture of *Gluconacetobacter xylinus* and *Lactobacillus mali*. Appl Microbiol Biotechnol 2006;73:915–21. https://doi.org/10.1007/s00253-006-0515-2.
[14] Tsuji A, Kaneko Y, Takahashi K, Ogawa M, Goto S. The effects of temperature and pH on the growth of eight enteric and nine glucose non-fermenting species of gram-negative rods. Microbiol Immunol 1982;26:15–24. https://doi.org/10.1111/j.1348-0421.1982.tb00149.x.
[15] Allesen-Holm M, Barken KB, Yang L, Klausen M, Webb JS, Kjelleberg S, Molin S, Givskov M, Tolker-Nielsen T. A characterization of DNA release in *Pseudomonas aeruginosa* cultures and biofilms. Mol Microbiol 2006;59:1114–28. https://doi.org/10.1111/j.1365-2958.2005.05008.x.
[16] Mugunthan S, Li Wong L, Winnerdy FR, Summers S, Bin Ismail MH, Foo YH, JaggI TK, Meldrum OW, Tiew PY, Chotirmall SH, Rice SA, Phan AT, Kjelleberg S, Seviour T. RNA is a key component of extracellular DNA networks in *pseudomonas aeruginosa* biofilms. Nat Commun 2023;14. https://doi.org/10.1038/s41467-023-43533-3.
[17] Whitchurch CB, Tolker-Nielsen T, Ragas PC, Mattick JS. Extracellular DNA required for bacterial biofilm formation. Science 2002;295:1487. https://doi.org/10.1126/science.295.5559.1487.
[18] Turnbull L, Toyofuku M, Hynen AL, Kurosawa M, Pessi G, Petty NK, Osvath SR, Cárcamo-Oyarce G, Gloag ES, Shimoni R, Omasits U, Ito S, Yap X, Monahan LG, Cavaliere R, Ahrens CH, Charles IG, Nomura N, Eberl L, Whitchurch BC. Explosive cell lysis as a mechanism for the biogenesis of bacterial membrane vesicles and biofilms. Nat Commun 2016;7. https://doi.org/10.1038/ncomms11220.
[19] Okshevsky M, Regina VR, Meyer RL. Extracellular DNA as a target for biofilm control. Curr Opin Biotechnol 2015;33:73–80. https://doi.org/10.1016/j.copbio.2014.12.002.
[20] Jennings LK, Storek KM, Ledvina HE, Coulon C, Marmont LS, Sadovskaya I, Secor PR, Tseng BS, Scian M, Filloux A, Wozniak DJ, Howell PL, Parsek MR. Pel is a cationic exopolysaccharide that cross-links extracellular DNA in the *Pseudomonas aeruginosa* biofilm matrix. Proc Natl Acad Sci U S A 2015;112(36):11353–8. https://doi.org/10.1073/pnas.1503058112.
[21] Seviour T, Winnerdy FR, Li Wong L, Shi X, Mugunthan S, Hwee Foo Y, Castaing R, Adav SS, Subramoni S, Shewan HM, Stokes JR, Rice SA, Phan AT, Kjelleberg S. The biofilm matrix scaffold of *Pseudomonas aeruginosa* contains G-quadruplex extracellular DNA structures. npj Biofilms Microbiomes 2021;7:27. https://doi.org/10.1038/s41522-021-00197-5.
[22] Buzzo JR, Devaraj Aishwarya, Gloag ES, Jurcisek JA, Robledo-Avila F, Kesler T, Wilbanks K, Mashburn-Warren L, Balu S, Wickham J, Novotny LA, Stoodley P, Bakaletz LO, Goodman SD. Z-form extracellular DNA is a structural component of the bacterial biofilm matrix. Cell 2021;184(23):5740–58. https://doi.org/10.1016/j.cell.2021.10.010.
[23] Schramm MJ, Hestrin S. Factors affecting production of cellulose at the air/liquid interface of a culture of *Acetobacter xylinum*. J Gen Microbiol 1954;111:123–9.
[24] George J, Ramana KV, Sabapathy SN, Jagannath JH, Bawa AS. Characterization of chemically treated bacterial (*Acetobacter xylinum*) biopolymer: some thermo-mechanical properties. Int J Biol Macromol 2005;37:189–94. https://doi.org/10.1016/j.ijbiomac.2005.10.007.
[25] Hestrin S, Schramm M. Synthesis of cellulose by *Acetobacter xylinum*. II. Preparation of freeze-dried cells capable of polymerizing glucose to cellulose. Biochem J 1954;58:345–52. https://doi.org/10.1042/bj0580345.
[26] Usha Rani M, Udayasankar K, Anu Appaiah KA. Properties of Bacterial cellulose produced in grape medium by native Isolate *Gluconacetobacter* Sp. J Appl Polym Sci 2011;120:2835–41.
[27] Khan S, Ul-Islam M, Khattak WA, Ullah MW, Park JK. Bacterial cellulose-poly(3,4-ethylenedioxythiophene)-poly(styrenesulfonate) composites for optoelectronic applications. Carbohydr Polym 2015;127:86–93. https://doi.org/10.1016/j.carbpol.2015.03.055.
[28] Movasaghi Z, Rehman S, Rehman I. Fourier transform infrared (FTIR) spectroscopy of biological tissues. Appl Spectrosc Rev 2008;43:134–79. https://doi.org/10.1080/05704920701829043.
[29] Dai F, Zhuang Q, Huang G, Deng H, Zhang X. Infrared spectrum characteristics and quantification of OH groups in coal. ACS Omega 2023;8(19):17064–76. https://doi.org/10.1021/acsomega.3c01336.
[30] Liu K, Catchmark JM. Enhanced mechanical properties of bacterial cellulose nanocomposites produced by co-culturing *Gluconacetobacter hansenii* and *Escherichia coli* under static conditions. Carbohydr Polym 2019;219:12–20. https://doi.org/10.1016/j.carbpol.2019.04.071.
[31] Parker AW, Quinn SJ. Infrared spectroscopy of DNA. In: Roberts GCK, editor. Encyclopedia of biophysics. Berlin, Heidelberg: Springer; 2013. https://doi.org/10.1007/978-3-642-16712-6_112.

[32] Teodoro KBR, Silva MJ, Andre RS, Schneider R, Martins MA, Mattoso LHC, Correa DS. Exploring the potential of cellulose autofluorescence for optical detection of tannin in red wines. Carbohydr Polym 2024;324. https://doi.org/10.1016/j.carbpol.2023.121494.

[33] Wilton M, Halverson TWR, Charron-Mazenod L, Parkins MD, Lewenza S. Secreted phosphatase and deoxyribonuclease are required by *Pseudomonas aeruginosa* to defend against neutrophil extracellular traps. Infect Immun 2018;86:9. https://doi.org/10.1128/IAI.00403-18.

[34] Fang L, Catchmark JM. Characterization of cellulose and other exopolysaccharides produced from *Gluconacetobacter* strains. Carbohydr Polym 2015;115:663–9. https://doi.org/10.1016/j.carbpol.2014.09.028.

[35] Rubio-Canalejas A, Baelo A, Herbera S, Blanco-Cabra N, Vukomanovic M, Torrents E. 3D spatial organization and improved antibiotic treatment of a *Pseudomonas aeruginosa–Staphylococcus aureus* wound biofilm by nanoparticle enzyme delivery. Front Microbiol 2022;13. https://doi.org/10.3389/fmicb.2022.959156.

[36] Chakraborty J, Mallick S, Raj R, Das S. Functionalization of extracellular polymers of *Pseudomonas aeruginosa* N6P6 for synthesis of cdS nanoparticles and cadmium bioadsorption. J Polym Environ 2018;26:3097–108. https://doi.org/10.1007/s10924-018-1195-6.

[37] Ju X, Bowden M, Brown EE, Zhang X. An improved X-ray diffraction method for cellulose crystallinity measurement. Carbohydr Polym 2015;123:476–81. https://doi.org/10.1016/j.carbpol.2014.12.071.

[38] Segal L, Creely JJ, Martin AE, Conrad CM. An empirical method for estimating the degree of crystallinity of native cellulose using the X-Ray diffractometer. Textil Res J 1959;29:786–94. https://doi.org/10.1177/004051755902901003.

[39] Gao M, Li J, Bao Z, Hu M, Nian R, Feng D, An D, Li X, Xian M, Zhang H. A natural in situ fabrication method of functional bacterial cellulose using a microorganism. Nat Commun 2019;10:437. https://doi.org/10.1038/s41467-018-07879-.